Impact of plants obscuration on energy balance: Theoretical and numerical study

Mohamed-Amine Kenai, Laurent Libessart, Stephane Lassue, Didier Defer

Impact of plants obscuration on energy balance: theoretical and numerical study

Kenai Mohamed-Amine[a], Libessart Laurent[b*], Lassue Stephane[b], Defer Didier[b]

[a]*YNCREA-Ecole des Hautes Etudes d'Ingénieur, LGCgE, F-59000 Lille, France*

[b]*Univ. Artois, EA 4515, Laboratoire de Génie Civil et géo-Environnement (LGCgE), F-62400 Béthune, France*

[*]Corresponding author: Laurent Libessart, laurent.libessart@univ-artois.fr

Abstract

This paper presents the evaluation of the energy effect of a solar mask created by a vegetalized wall on the thermal performance of a building envelope in a temperate climate. The paper describes mainly the adaptation of a simplified prediction model. The method remains similar to the occultation by an artificial material, however, some considerations related to the plants characteristics was incorporated such as: the semi-transparent aspect of the foliage plants and their geometrical distribution. The simplified model has been developed and validated on the basis of tests carried out with a controlled occultation experimental set-up. This device was then used for the experimental monitoring of the impact of two types of plant: ivy and Virginia creeper. The coverage rate was determined using an image analysis process, which allowed the comparison of the tests with the theoretical results. The numerical prediction was very close to the experimental values, and the average error was about 1.5°C. Finally, an experimental analysis of the effects of deciduous plants and another evergreen was carried out. The deciduous plant allowed the facade to benefit from solar radiation in winter. While the persistent leaves have better limited summer overheating.

Keywords: vegetalized walls, obscuration effect, model adaptation, thermal effect analysis.

Nomenclature

Symbols :

T	temperature, K
VW	vegetalized wall
$Is^{\downarrow}$	incident solar radiation, W/m²
$Ir^{\downarrow}$	infrared radiation, W/m²
c_p	specific heat, $J.kg^{-1}.K^{-1}$
d_0	height of movement, m
df	average leaf thickness, m
F	leaf cover index
h_{cv}	convective exchange coefficient, $W.m^{-2}.K^{-1}$
hf	height of vegetal canopy, m
k	constant of Von Karman
ra	aerodynamic resistance, $s.m^{-1}$
rc	« resistance » to sensible thermal transfer, $s.m^{-1}$
uc	flow velocity within the plant layer, m/s
U_m	wind speed, m/s
z_{0H}	roughness lengths « sensitive heat », m
z_{0m}	roughness lenghts «amount of movement», m

Greek letters :

α	solar absorption coefficient
β_{zen}	solar zenith angle
φ	flux density, W/m²
σ	constant of Stefan-Boltzmann, $5.67\times10^{-8} W/m^2.K^4$
σ_{occ}	coverage rate, [0,1]
ε	emissivity, [0,1]
τ	transmissivity, [0,1]
σ_{vw}	coverage rate, [0,1]
μ^*	solar extinction coefficient

Indices / Exponents :

CC	cellular concrete
vw	vegetalized wall
Eq	equivalent
sol	solar
R_{env}	infrared exchanges with the environment
R_{occ}	infrared exchanges with the VW
R_{env}	infrared exchanges with the environment
R_{occ}	infrared exchanges with the VW
$R_{env\text{-}vw}$	infrared exchanges with the environment
$R_{cc\text{-}vw}$	infrared exchanges with the vegetalized wall
cv	convection
tr	transmitted
th	theoretical
AG	air gap
SWR	short-wave radiation, W/m²
LWR	long-wave radiation, W/m²

1. Introduction

The issue of reducing energy consumption is a major factor in solving contemporary environmental problems. From the first world conference on the environment (Stockholm, 1972) to the recent climate conference (Cop 21, Paris 2015), passing by the Kyoto agreements (1997) and the various inter-state negotiations around the world, the building sector has been identified as one of the most important targets on which energy saving efforts must be made [1]. The vegetation of building envelop by creating Vegetalized Walls or Vegetal Walls (VW) is among the various solutions for the optimization of energy consumption in buildings and some well mediatised projects have given a very good image of the process (Quai Branly Museum in Paris for example [2]). This tendency mainly came from Germany in the early 1970s. Although it is a very old technique, the main driver of its

development remains, to this day, the aesthetic aspect and the desire to provide originality to buildings [3]. However, green walls can also have very positive effects on the improvement of the sound insulation [4–6] and the thermal performance of buildings [7–16]. According to numerous studies, green walls contribute to the improvement of air quality [17–21], bring biodiversity to urban centres and limit the development of the heat island phenomenon [22–25].

It is notable, however, that up to now there are very few studies proposing tools for evaluating the thermal effects of green walls on buildings [26].

The experiment have shown the effect of a masking made by an artificial material [27]. A simplified model was developed on the basis of this experiment, which allowed the theoretical evaluation of the thermal impact of an artificial masking according to its coverage rate. The artificial masking device was replaced by real vegetation and the theoretical study was supplemented by a model, which is more adapted to the case of masking by vegetation. The natural growth of the plants was evaluated by an image processing method, which made it possible to determine the coefficient of the coverage rate [27]. The differences between artificial masking and another with plants are discussed and interpreted as new parameters in the different equations. This work aims to evaluate the thermal impact of "simple" VW by numerical and theoretical tools. The paper presents the modelling of the thermal effect of plants on buildings at prototype and real scale.

2. Methods

2.1. Experimental approach

This part presents the evaluation of the energy effect of a solar mask created by a VW [27]. The aim was to evaluate the impact of vegetation on the thermal performance of building envelope under a temperate climate, in summer and winter. This wall was equipped with a device simulating the masking effect of a vegetal cover by an artificial material. This approach allowed the listing and evaluation of the principal transfer phenomena that occur between the wall and its environment. Thus, a relatively simplified model has been validated from the comparison between numerical simulations and experimental results obtained for the thermal labs which are under natural constraints. These cubic cells of reduced size each consisted of five thermally insulated walls and a test wall, facing south, equipped with heat flux and temperature sensors (see detailed description on part 1). They are now equipped with vegetalized walls (Fig.1). The central prototype "Lab1" serves as a reference, while Lab2 and Lab3 are respectively equipped with an evergreen (Ivy) plant and a deciduous plant (Virginia creeper).

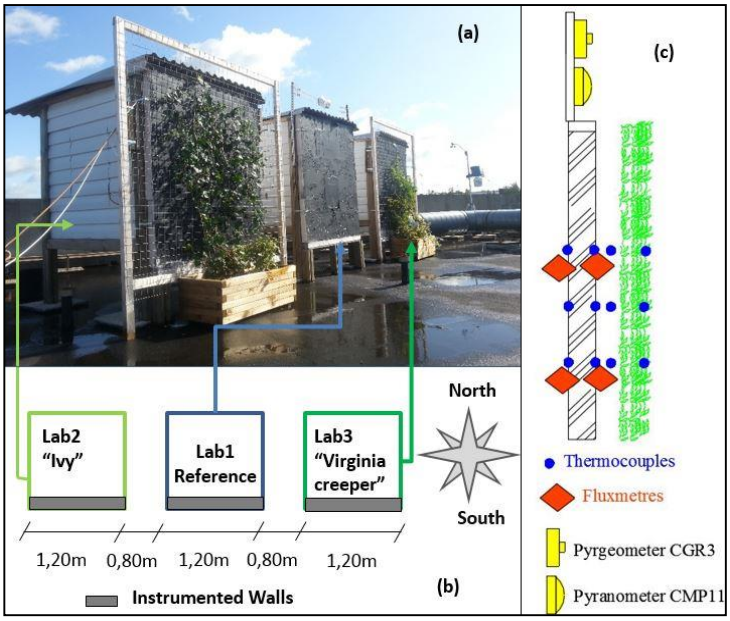

Fig. 1: Test of masking by the vegetation ; (a) general view ; (b) distribution of vegetated walls ; (c) sensors disposition.

The experimental results [27] showed clearly the effect of masking on reducing surface and air temperatures. It was found a significant decrease in the thermal heat flux through the south oriented wall depending on the increase of the coverage rates.

2.2. Preliminary Theoretical model

A preliminary theoretical model has been developed to identify the parameters that affect the heat flow received by an occult wall. This model was created by performing an energy balance to determine the heat flux resulting from various transfer phenomena between the outer wall and the environment, which are conditioned by the presence of a partial occultation (Fig. 2).

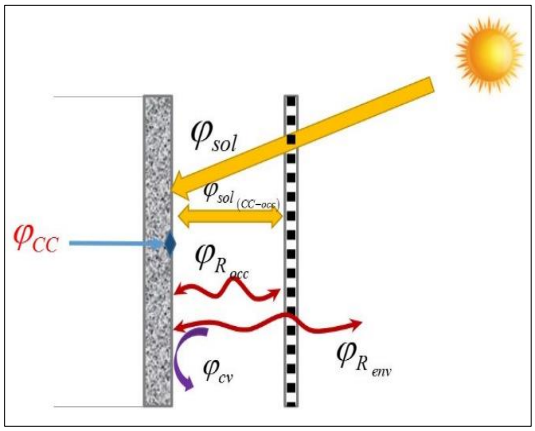

Fig. 2: Energy balance at the outer surface of the CC wall.

2.2.1. Energy exchange balance

The heat flux at the outer wall (φcc) obtained by the balance of the radiative and convective exchanges SWR and LWR, can be written in the following form:

$$\varphi_{CC} = \varphi_{sol} - \varphi_{R_{env}} - \varphi_{R_{occ}} - \varphi_{cv} \quad (1)$$

The different terms of the energy exchange balance at the CC wall are detailed below (2.2.2. to 2.2.4.). The transfer equations used are relatively standard in the bibliography [28], the characteristic term of the coverage rate was added here in correspondence with our study. The radiative characteristics of each of the materials used are given in Table 2.

Table 2 : Radiative properties

Radiative Properties	α [0/1]	ε [0/1]	τ [0/1]	r [0/1]
Wall CC	0.9	0.9	0	0.1
Masking	0.9	0.9	0	0.1

Calculations were made using meteorological records and measured temperatures on the CC wall surfaces, within the shading device and the air gap.

2.2.2. Solar radiation

The radiation absorbed by the outer surface of the wall is equal to the difference between the radiation which passes through the uncovered part of the occultation $Is^{\downarrow}.(1-\sigma_{occ})$ and the radiation reflected by the wall.

$$\varphi_{sol} = \alpha_{CC}\left(1-\sigma_{occ}\right)\times Is^{\downarrow} \quad (2)$$

The SWR radiative exchanges between the masking and the outer surface of the cellular concrete are represented by the solar radiation of equation (2), and equation (3) takes into account possible multiple reflections between the wall and the inner surface of the masking.

$$\varphi_{sol_{(occ-CC)}} = Is^{\downarrow}.\alpha_{CC}\,(1-\sigma_{occ})\times\sum_{n=2}^{\infty} r_{CC}^{n}(\sigma_{\mathrm{occ}}.\,r_{occ})^{n-1} \quad (3)$$

The value of n = 2 is largely sufficient here, the surfaces having high solar absorption coefficients (close to 0.9).

2.2.3. Infrared radiation

The radiation (LWR) at the CC wall is the sum of the exchanges between the wall and the environment is $\left(\varphi_{R_{env}}\right)$, and between the wall and the masking is $\left(\varphi_{R_{occ}}\right)$.

$$\varphi_{R_{env}} = \frac{\varepsilon_{CC}\sigma.\left(T_{CC}^4 - T_{EQ}^4\right)\times\left(1-\sigma_{occ}\right)}{1-\sigma_{occ}.\left(1-\varepsilon_{CC}\right)} \quad (4)$$

The exchanges between the CC wall and the environment are calculated from an equivalent temperature determined using a pyrgeometer placed on a vertical wall and which integrates the combined effect of the "surfaces" constituting the radiative environment at low temperatures (sky, ground, etc.). The equivalent temperature is obtained by equation (5).

$$T_{EQ} = \left(\frac{Ir}{\sigma}\right)^{\frac{1}{4}} \quad (5)$$

The radiative exchanges LWR between the masking and the CC wall are represented by the following equation:

$$\varphi_{R_{occ}} = \frac{\sigma.\left(T_{CC}^4 - T_{occ}^4\right)}{\frac{1-\varepsilon_{CC}}{\varepsilon_{CC}} + \frac{1}{\sigma_{occ}} + \frac{1-\varepsilon_{occ}}{\varepsilon_{occ}} \times \frac{1}{\sigma_{occ}}} \quad (6)$$

2.2.4. Convection

The heat flux exchanged by convection (φ_{cv}) is given by the following equation:

$$\varphi_{cv} = h_{cv}.\left(T_{CC} - T_{\mathrm{AG}}\right) \quad (7)$$

The convective heat exchange coefficient h_c was determined from the correlation used by [29]:

$$h_{cv} = 1.31.\left|T_{CC} - T_{\mathrm{AG}}\right|^{\frac{1}{3}} + 9 \quad (8)$$

The constant 9 of the last equation is an experimental factor recommended to take into account the effect of the average wind speed.

2.3. Equations resolution

The equations composing the energy balance at the outer surface of the cellular concrete wall (4), (6) and (8) involve nonlinear terms according to the surface temperature of the cellular concrete wall (Tcc).

A resolution of the energy balance equations was performed under Matlab using the Newton-Raphson method. Thus, for each time step, the "theoretical" calculated temperature of the wall surface is evaluated numerically with an iterative calculation. Once this temperature is approximated with an error deemed as acceptable, the program resets the inputs to make the approximation in the next time step and so on, until the last time step entered for the end of the calculations (Fig. 3).

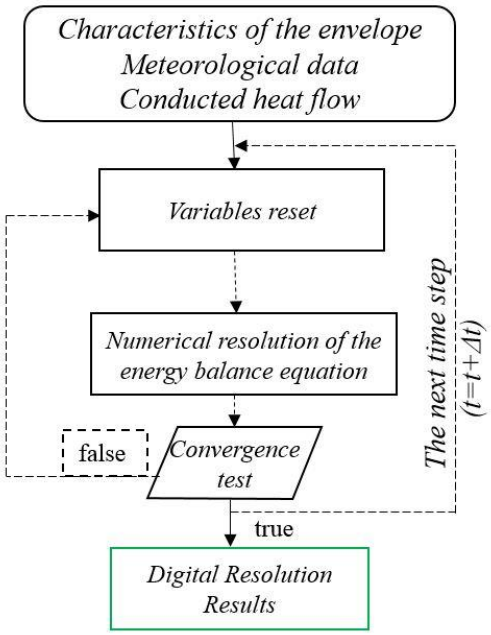

Fig. 3: Diagram of the resolution algorithm.

For the operation of the algorithm (Fig. 3), it is necessary to introduce the characteristics of the envelope and the meteorological data. The heat flux on the outer surface of the cellular concrete wall must also be provided at each time step in order to evaluate the temperature. The temperatures evaluated with this algorithm are validated experimentally in the following section.

2.4. Preliminary model validation

A comparison between the theoretical temperatures, represented in orange (T°_theoretical) and the measured temperatures, in blue (T°_measured) was carried out for the different coverage rates (0-100%) in order to validate the preliminary model based on the energy balance equations in the artificial occultation test (Fig. 4).

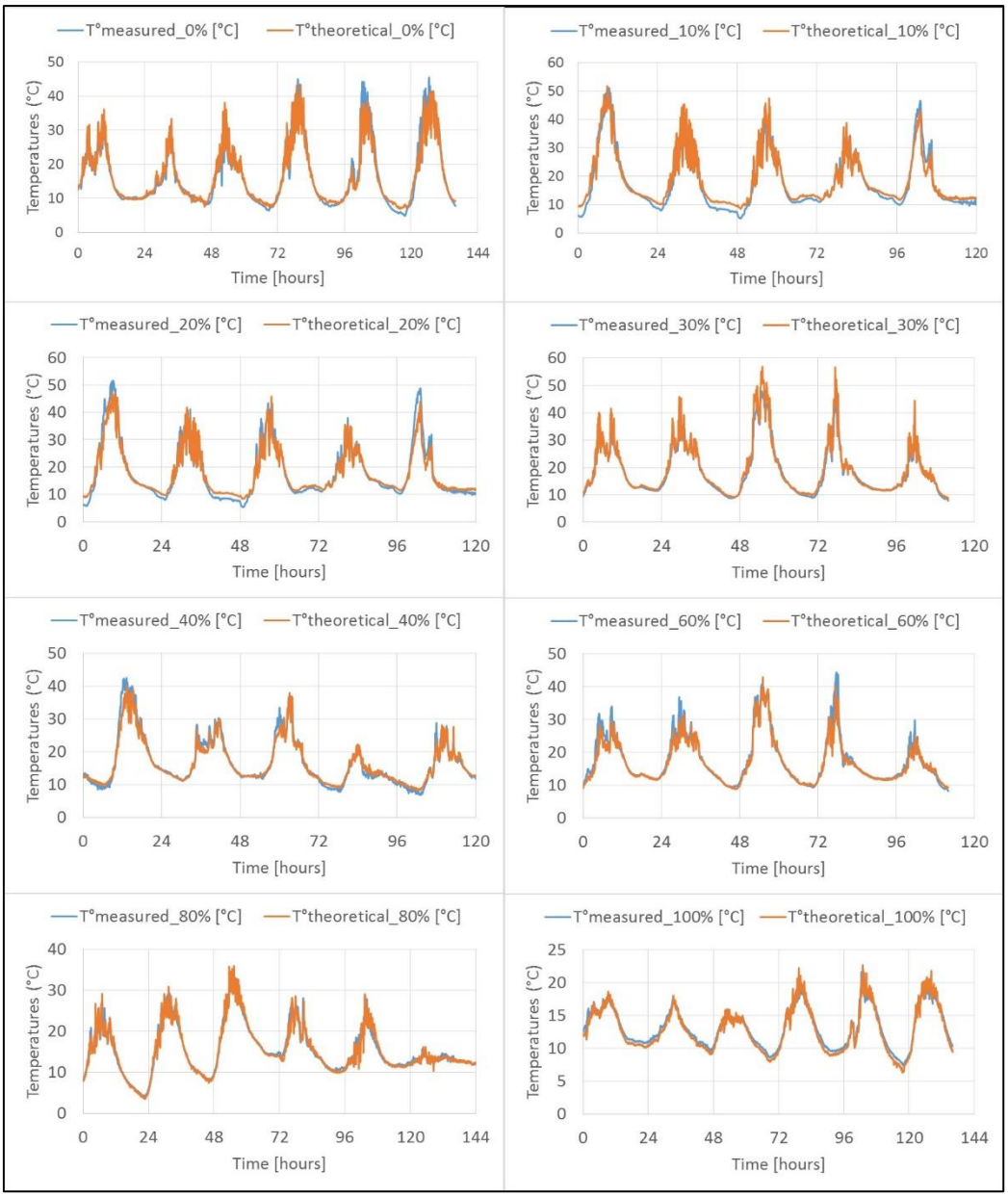

Fig. 4: Comparison of numerical and experimental results.

For all coverage rates, the theoretical model closely reproduces the measured temperature. For example, in the case of coverage rates of 100%, the mean deviation between the theoretical temperatures curve and the experimental curve for a period of 6 days was 0.54 °C.

A typical day was selected to better illustrate the comparison between the numerical results and the experimental results. The coverage rate during this typical day (12/05/2014) was 50% on the lab3, and the meteorological data used for the chosen day are shown in Fig. 5.

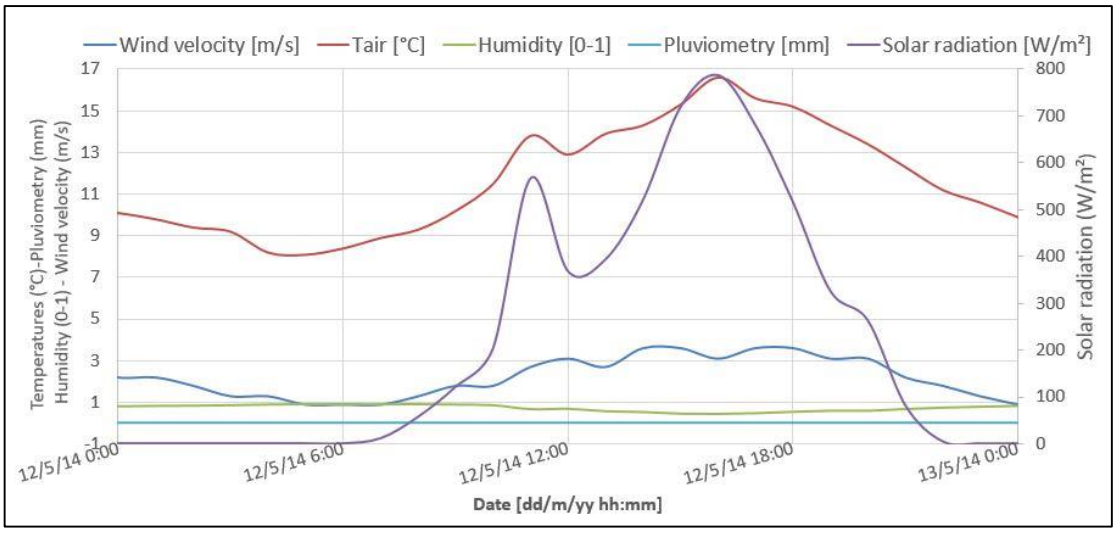

137

138 **Fig. 5:** Meteorological data.

139 This typical day was selected according to the maximum temperature values and the solar radiation recorded
140 during the period of the test of the controlled occultation rate. The peak of solar radiation was 786 W/m² at
141 16h00, while the ambient air temperature was around a maximum of 16.6°C for the period and a minimum of
142 8.1°C recorded at 5h00. No precipitation was observed during this day, but high humidity values were recorded
143 during the night and in the morning (82% to 90% between 1h00 and 10h00). The wind speed was relatively low
144 during the selected sequence (0.9 to 3.6 m/s).

145 The results of validation of the theoretical model during the typical sequence are illustrated in Fig. 6.

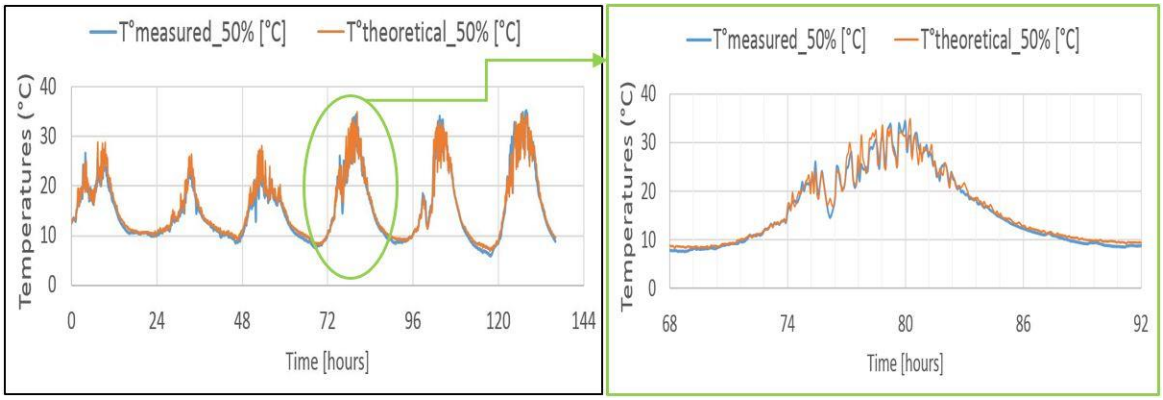

146

147 **Fig. 6 :** Comparison between theoretical and measured temperatures (σocc=50%).

148 In this figure, it is observed that the calculated heat flux is globally similar to that which is measured. The mean
149 deviation between the theoretical and measured temperature is of the order of 1.3°C. Deviations of up to 3.8°C
150 were recorded during peaks and in the rapid changes in solar radiation. These deviations coincide with the period
151 when solar radiation is rapidly changing from 500 to 786 W/m². During the night and in the morning, the
152 deviations are relatively higher than the mean values, they correspond perfectly to the sequence in which, the

relative humidity was very high and the solar radiation not exceeding 200 W/m².

Despite these few deviations corresponding to particular sequences (high humidity and rapid change of solar radiation), the influence of the coverage rate was reproduced fairly accurately throughout the test.

The good similarity obtained, between the theoretical model and the experimental results, allowed an appropriate validation of the controlled occultation model. The equations of this model will be used as a basis for the modelling of the behaviour of the vegetalized walls.

2.5. Adaptation of equations to the case of vegetation

The energy balance at a wall obscured by vegetation is based on the balance equations of solar radiation exchanges, infrared exchanges and convective exchanges (Equation 9).

$$\varphi_{cc} = \varphi_{sol} - \varphi_{R_{env-CC}} - \varphi_{R_{vw-BC}} - \varphi_{cv} \quad (9)$$

Among the major differences between the two types of occultation is the semi-transparent foliage aspect of plants. This involves a new equation quantifying the solar flux (φ_{sol-tr}) which crosses the "vegetation cover" and involves several and numerous parameters (only parameters related to the obscuration effect are treated) (Fig. 7).

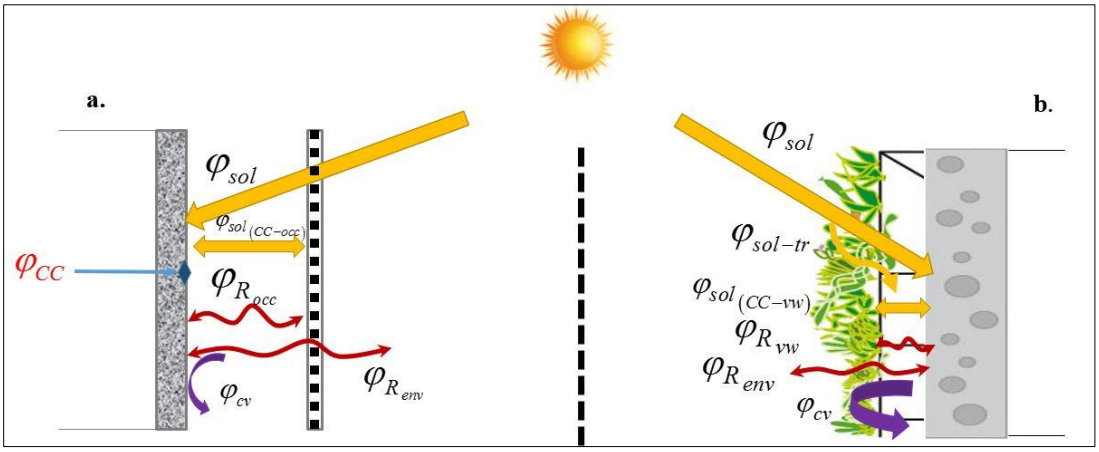

Fig. 7: Elements of the energy balance ;(a) case of artificial obscuration ; (b) case of masking by the vegetation.

The second important difference is related to the geometry of the occultation. In the experiment, realized with artificial occultation, the objective was to master the role of the coverage rate. This has been possible by using a relatively simple structure where each of the meshes of the occultation lies in the same plane and thus in two dimensions (2D). In the case of vegetation, the leaves of the plants replace the square meshes. The distribution of plant leaves is not limited by a 2D plan. The thickness of the leaf layer, the density and the number of leaves are new parameters to be integrated into the energy balance equations. This last aspect requires modification of the

transmitted and absorbed solar radiation and an adaptation of the equations of convective exchanges. These convective exchanges are considered in the case of the artificial occultation to be similar to exchanges between two flat surfaces. They are more complex in the case of plants, and it is then necessary to take into account an aerodynamic resistance in the external surface area of the leaf layer and a resistance to the sensible heat transfer within the canopy layer, following its thickness, and the density of leaves.

2.5.1. Radiative exchanges

The radiative exchanges balance was adapted according to the characteristics of the plants, no change was made to the infrared radiation equations between the cellular concrete wall (W_{CC}) and the environment (Equation 10) on one hand and between the VW and the W_{CC} on the other hand (Equation 11):

$$\varphi_{R_{CC-env}} = \frac{\varepsilon_{BC}\sigma \times \left(T_{CC}^4 - T_{EQ}^4\right) \times \left(1-\sigma_{vw}\right)}{1-\sigma_{vw} \times \left(1-\varepsilon_{CC}\right)} \quad (10)$$

$$\varphi_{R_{vw-CC}} = \frac{\sigma \times \left(T_{CC}^4 - T_{vw}^4\right)}{\frac{1-\varepsilon_{CC}}{\varepsilon_{CC}} + \frac{1}{\sigma_{vw}} + \frac{1-\varepsilon_{vw}}{\varepsilon_{vw}} \times \frac{1}{\sigma_{vw}}} \quad (11)$$

Since the leaf layer of plants is considered semi-transparent to solar radiation, a transmitted flux term has been added (φ_{sol-tr}). This adds to the direct solar flux and to those exchanged between the masking and the W_{CC} have been expressed respectively by (φ_{sol}) and ($\varphi_{sol_{(vw-CC)}}$) in equations (12, 13).

$$\varphi_{sol} = \alpha_{CC}\left(1-\sigma_{vw}\right) \times Is \quad (12)$$

$$\varphi_{sol_{(vw-CC)}} = Is^{\downarrow} \times \alpha_{CC}\left(1-\sigma_{vw}\right) \times \sum_{n=2}^{\infty} r_{CC}^{n}\left(\sigma_{vw} \times r_{vw}\right)^{n-1} \quad (13)$$

The radiative flux transmitted by the foliar layer of plants (φ_{sol-tr}), is obtained as a function of the incident solar radiation, the W_{CC} absorption coefficient, the coverage rate of the plant layer and the solar transmission coefficient of the leaf layer (Equation 14).

$$\varphi_{sol-tr} = Is^{\downarrow} \times \alpha_{CC} \times \sigma_{CC} \times \tau_{vw} \quad (14)$$

The foliar solar transmission coefficient τ, is determined according to a simplified approach which consists in assuming the foliar layer as a homogeneous medium in which the radiation is absorbed and not diffused. With this assumption, the Beer-Lambert law can then describe the exponential attenuation of the radiation passing

through the leaf layer [23, 30]. Thus, the coefficient (τ_{vw}) is calculated as a function of the solar zenith angle (β_{zen}), the leaf coverage index (F) and a solar extinction coefficient (μ*) which vary according to the radiative properties of the leaves and their mean inclination (Equation 15).

$$\tau_{vw} = \exp\left(-\mu^* \times \beta_{zen} \times F\right) \quad (15)$$

The inclination of the leaves and the radiative properties of the plants (μ *) determine the depth up to which direct solar radiation (of β zenith angle) can penetrate in the leaf layer without being intercepted. The foliar cover index (F), for its part, is a dimensionless quantity, representing the spatial distribution of the leaf structure in three dimensions. In other words, the index F is taken to be equal to the coverage rate in the case of a spatial distribution in 2D only (case of artificial occultation). It is defined as the ratio between half of the total surface area of the leaves (up and down seeds) and the total surface area (CC wall). Unlike the coverage rate, which is limited to the ratio between the covered area and the total area, the index F is calculated taking into account the total number of leaves, even if they are superimposed (Equation 16).

$$F = \frac{1/2 \ Total\ leaf\ area}{W_{cc}\ area} \quad (16)$$

2.5.2. Convective exchanges

The new model of convective exchanges is inspired by the model validated by [23]. It is expressed as a function of an aerodynamic resistance of the top layer of the plants (ra) and a resistance to the sensible heat transfer (rc) within the foliage. The introduction of the two "resistances" (in $s.m^{-1}$) is similar to that which is generally used for the modelling of heat transfer by electrical analogy. The new convective flux at the level of the leaf layer, involving these two resistances, is given by the following equation:

$$\varphi_c = \frac{\rho_{air} \times cp_{air}}{rc + ra}\left(T_{CC} - T_f\right) \quad (17)$$

The aerodynamic resistance (ra) is defined by the variation of the wind speed above a rough surface. It is determined according to a general model often used by climatologists to describe the wind velocity profile at the upper boundary layer of a plant canopy [31, 32]. According to [23], the aerodynamic resistance (ra) which takes into account the very small deviations between the ambient air temperature and the foliage temperature can be calculated by equation (18):

$$ra = \frac{\left[\ln\left(\frac{(z_U - d_0)}{z_{0m}}\right)\right] \times \left[\ln\left(\frac{(z_U - d_0)}{z_{0H}}\right)\right]}{k^2 um} \quad (18)$$

With (k) the Von Karman constant (k$\approx$ 0.40) and (u_m) the wind speed measured at the distance (z_U). Whereas, the displacement height (d_0) and the roughness lengths (z_{0H}) and (z_{0m}) are calculated, according to [33], as a function of the height of the plant canopy (h_f) :

$$\begin{aligned} d_0 &= 0.701 h_f{}^{0.975} \\ z_{0m} &= 0.131 h_f{}^{0.997} \\ z_{0H} &= 0.1 z_{0m} \end{aligned} \quad (19)$$

The resistance to sensible heat transfer (rc) intervenes inside the plant layer. It is determined as a function of the velocity of the air flow within the plant canopy (uc) using the relationship below [34–36]:

$$rc = \frac{1}{0.004 + 0.012\ uc} \quad (20)$$

The air flow velocity within the plant layer (uc) is reduced as function of a specific coefficient of the vegetation layer (a) and is determined according to the following equation:

$$uc = \left[um.\ln\left(\frac{(h_f - d0)}{z_{0m}}\right) \Big/ \ln\left(\frac{(zU - d0)}{z_{0H}}\right)\right].e^{-a\left(1-\frac{0.05}{hf}\right)} \quad (21)$$

The coefficient (a) (in eq (21) is calculated according to the foliar surface index (F), the height of the plant canopy (hf) and the average leaves thickness (df):

$$a = \sqrt{0.2F.\frac{h_f}{d_f}} \quad (22)$$

Henceforth, the different equations used in the first part have been adapted to the case of vegetation. They will be validated after the determination of the coverage rate by an image analysis method.

3. Experimental validation

The different equations having the wall surface temperature (T_{CC}) as unknown parameter were solved with the Newton Raphson method. Then, in order to verify the relevance of the theoretical model, the results of the calculations were compared with the experimental measurements [27]. The parameters used in the theoretical modelling are grouped in table 1.

Table 1: Parameters for experimental validation

Parameters	Value	Parameters	Value
α_{CC}	0.90	ε_{CC}	0.96
σ_{vw}	0.45	σ	5.67 10^{-8}
r_{CC}	0.1	ε_{vw}	0.95
r_{vw}	0.3	h_f	0.15
$\mu*$	0.75	d_f	0.001
F	3		

The experimental data used for validation were recorded by the mini thermal lab at the end of the summer period of 2014.The meteorological data entered as inputs to the program are: ambient air temperature, short-wave solar radiation, equivalent environmental temperature and wind speed. In addition, data on precipitation and relative humidity are given only for information. These additional data may be useful for understanding numerical prediction errors, which generally coincide with possible rapid changes in the values for these two parameters (Fig. 8).

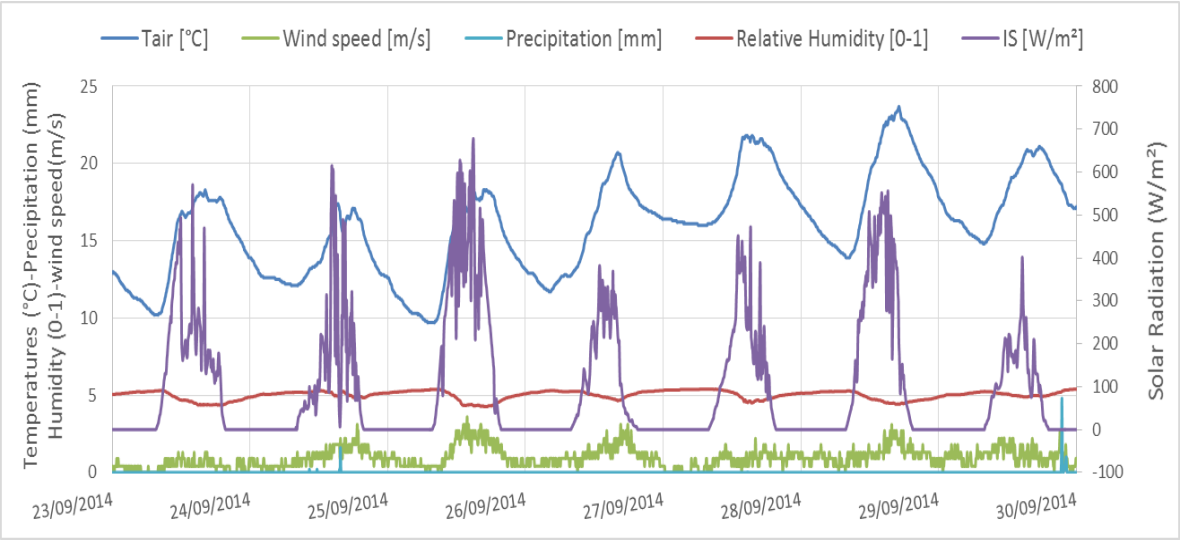

Fig. 8: Meteorological data of the validation sequence

During the sequence selected for experimental validation, the air temperature varied between 9 and 24°C. While the wind speed never exceeded 3.6 m/s over the entire validation sequence. As for solar radiation, the maximum values ranged between 400 and 700 W/m² with very rapid oscillations during the first three days of validation because of frequent cloud crossings.

The theoretical temperatures obtained for the surface of the CC wall were then compared with the outside surface temperatures recorded by the "Lab 2" (Fig. 9).

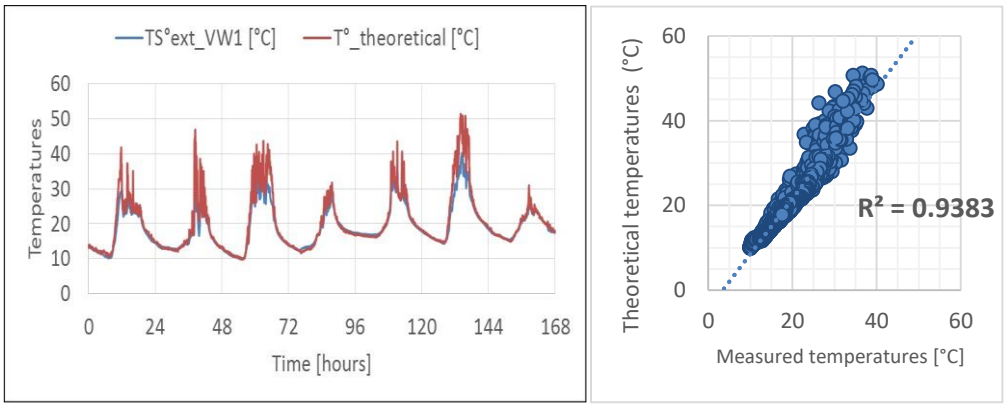

Fig. 9: Comparison of theoretical and measured temperatures

From the comparison, it appears that the numerical prediction is generally very close to the experimental values. The temperatures from the numerical calculations correspond to the experimental temperatures within about 1.5°C.

The average deviation observed corresponds to an average error of ± 6.4% throughout the validation sequence. However, it should be noted that the differences between the calculated and the measured temperatures are less than 1°C over 90% of the values. The error calculated on 90% of the values, which does not take into account the deviations due to the rapid variations of the solar radiation, is less than 4.7% (less than 1°C). This difference is very acceptable for validations under external conditions.

4. Conclusion

This work presents a new contribution to the numerical evaluation of the thermal effects of vegetalized walls. A preliminary theoretical model was established at the end of the experimental part and the overall heat flow behaviour under the imposed coverage rates was reproduced very correctly. The comparison between theoretical and experimental temperatures allowed the validation of the proposed model on small scale. The model will be improved and better adapted to the case of climbing plants and then integrated into a thermal building simulation software. This will enable the prediction of the effect of plants on the thermal behaviour of a real building under various climates. The modelling of the effects of the occultation by a vegetable screen was introduced by presenting the differences between a vegetable screen and the occultation by an artificial material. New equations incorporating these modifications have been added to the model established in the first part. Then, the results from the new model were compared with the experimental results. The relevance of the numerical model has been discussed through experimental confrontation.

The experimental and theoretical approaches undertaken, demonstrated the thermal interest of simple vegetalized walls and highlighted the complexity of the transfer phenomena within a plant layer. This will allow future

modelling of the thermal effect of plants on buildings at real scale. The developed digital tool made it possible to bring more precision on the effects of plants in regions with a temperate climate. It will also allow the study of the thermal effects of simple vegetalized walls in other climates and for different constructions.

Acknowledgement

This research was conducted out at the Laboratory of Civil Engineering and Geo-Environment of University of Artois, the Graduate School of Engineering HEI of Lille in the context of the project "Building and Positive Biodiversity" (2012- 2015), supported by the Catholic University of Lille, the "Nord-Pas-de-Calais" Regional Council and the European Metropolis of Lille.

References

[1] M.A. Kenai, Caractérisation, Analyse et Modélisation des Echanges Energétiques entre un Mur Végétalisé intensif et son environnement (in French), (Phd thesis), University of Artois, 2016.

[2] P. Blanc, Vertical garden Patrick Blanc. The Vertical garden, from nature to cities - a botanical and artistic approach by Patrick Blanc, (2005). http://www.verticalgardenpatrickblanc.com (accessed February 1, 2013).

[3] M. Köhler, Green facades—a view back and some visions, Urban Ecosystems. 11 (2008) 423–436. doi:10.1007/s11252-008-0063-x.

[4] Z. Azkorra, G. Pérez, J. Coma, L.F. Cabeza, S. Bures, J.E. Álvaro, A. Erkoreka, M. Urrestarazu, Evaluation of green walls as a passive acoustic insulation system for buildings, Applied Acoustics. 89 (2015) 46–56. doi:10.1016/j.apacoust.2014.09.010.

[5] T. Van Renterghem, D. Botteldooren, Reducing the acoustical façade load from road traffic with green roofs, Building and Environment. 44 (2009) 1081–1087. doi:10.1016/j.buildenv.2008.07.013.

[6] N.H. Wong, A.Y. Kwang Tan, P.Y. Tan, K. Chiang, N.C. Wong, Acoustics evaluation of vertical greenery systems for building walls, Building and Environment. 45 (2010) 411–420. doi:10.1016/j.buildenv.2009.06.017.

[7] S.W. Peck, C. Callaghan, B. Bass, M.E. Kuhn, GREENBACKS FROM GREEN ROOFS: FORGING A NEW INDUSTRY IN CANADA, 1999. http://commons.bcit.ca/greenroof/files/2012/01/Greenbacks.pdf.

[8] N.H. Wong, A.Y. Kwang Tan, Y. Chen, K. Sekar, P.Y. Tan, D. Chan, K. Chiang, N.C. Wong, Thermal evaluation of vertical greenery systems for building walls, Building and Environment. 45 (2010) 663–672. doi:10.1016/j.buildenv.2009.08.005.

[9] U. Mazzali, F. Peron, P. Romagnoni, R.M. Pulselli, S. Bastianoni, Experimental investigation on the energy performance of Living Walls in a temperate climate, Building and Environment. 64 (2013) 57–66. doi:10.1016/j.buildenv.2013.03.005.

[10] M. Haggag, A. Hassan, S. Elmasry, Experimental study on reduced heat gain through green façades in a high heat load climate, Energy and Buildings. 82 (2014) 668–674. doi:10.1016/j.enbuild.2014.07.087.

[11] R.W.F. Cameron, J. Taylor, M. Emmett, A Hedera green façade – Energy performance and saving under different maritime-temperate, winter weather conditions, Building and Environment. 92 (2015) 111–121. doi:10.1016/j.buildenv.2015.04.011.

[12] R. Djedjig, R. Belarbi, E. Bozonnet, Experimental study of green walls impacts on buildings in summer and winter under an oceanic climate, Energy and Buildings. 150 (2017) 403–411. doi:10.1016/j.enbuild.2017.06.032.

[13] R. Djedjig, E. Bozonnet, R. Belarbi, Analysis of thermal effects of vegetated envelopes: Integration of a validated model in a building energy simulation program, Energy and Buildings. 86 (2015) 93–103. doi:10.1016/j.enbuild.2014.09.057.

[14] Y. He, H. Yu, A. Ozaki, N. Dong, S. Zheng, An investigation on the thermal and energy performance of living wall system in Shanghai area, Energy and Buildings. 140 (2017) 324–335. doi:10.1016/j.enbuild.2016.12.083.

[15] E. Cuce, Thermal regulation impact of green walls: An experimental and numerical investigation, Applied Energy. 194 (2017) 247–254. doi:10.1016/j.apenergy.2016.09.079.

[16] T. Safikhani, M. Baharvand, Evaluating the effective distance between living walls and wall surfaces, Energy and Buildings. 150 (2017) 498–506. doi:10.1016/j.enbuild.2017.06.029.

[17] M. Ottelé, H.D. van Bohemen, A.L.A. Fraaij, Quantifying the deposition of particulate matter on climber vegetation on living walls, Ecological Engineering. 36 (2010) 154–162. doi:10.1016/j.ecoleng.2009.02.007.

[18] S. Wismer, L. Knowles, P. MacLean, M. Rosato, C. Stanley, S. Volpe, D. Yousif, Living Wall A Feasibility Study for the SLC, University of Wateroloo, 2002. http://environment.uwaterloo.ca/research/watgreen/projects/library/f02livingwall.pdf.

[19] S. Sheweka, A.N. Magdy, The Living walls as an Approach for a Healthy Urban Environment, Energy Procedia. 6 (2011) 592–599. doi:10.1016/j.egypro.2011.05.068.

[20] L. Kong, Z. Shi, L.M. Chu, Carbon emission and sequestration of urban turfgrass systems in Hong Kong,

Science of The Total Environment. 473 (2014) 132–138. doi:10.1016/j.scitotenv.2013.12.012.

[21] C. Gromke, A vegetation modeling concept for Building and Environmental Aerodynamics wind tunnel tests and its application in pollutant dispersion studies, Environmental Pollution. 159 (2011) 2094–2099. doi:10.1016/j.envpol.2010.11.012.

[22] E. Alexandri, P. Jones, Temperature decreases in an urban canyon due to green walls and green roofs in diverse climates, Building and Environment. 43 (2008) 480–493. doi:10.1016/j.buildenv.2006.10.055.

[23] R. Djedjig, Impacts des enveloppes végétales à l'interface bâtiment microclimat urbain (in French), (Phd thesis), University of La Rochelle, 2013.

[24] T. Susca, S.R. Gaffin, G.R. Dell'Osso, Positive effects of vegetation: Urban heat island and green roofs, Environmental Pollution. 159 (2011) 2119–2126. doi:10.1016/j.envpol.2011.03.007.

[25] E.J. Gago, J. Roldan, R. Pacheco-Torres, J. Ordóñez, The city and urban heat islands: A review of strategies to mitigate adverse effects, Renewable and Sustainable Energy Reviews. 25 (2013) 749–758. doi:10.1016/j.rser.2013.05.057.

[26] L. Libessart, M.A. Kenai, Measuring thermal conductivity of green-walls components in controlled conditions, Journal of Building Engineering, 19 (2018) 258-265. doi.org/10.1016/j.jobe.2018.05.016.

[27] M.A. Kenai, L. Libessart, S. Lassue, D. Defer, Impacts of plants occultation on energy balance : Experimental study, Energy and Buildings. 162 (2018) 208-2018. doi:10.1016/j.enbuild.2017.12.024.

[28] A.-M. Bianchi, Y. Fautrelle, J. Etay, Transferts thermiques, 1ère édition, PPUR, 2004.

[29] J.M. Blanco, P. Arriaga, E. Roji, C. Cuadrado, Investigating the thermal behavior of double-skin perforated sheet façades: Part A: Model characterization and validation procedure, Building and Environnement. 82 (2014) 50–62. doi:10.1016/j.buildenv.2014.08.007.

[30] J.L. Monteith, M.H. Unsworth, Principles of Environmental Physics, 4th ed., Academic Press, 2013. http://denning.atmos.colostate.edu/readings/Monteith.and.Unsworth.4thEd.pdf.

[31] W.P. Kustas, B.J. Choudhury, K.E. Kunkel, L.W. Gay, Estimate of the aerodynamic roughness parameters over an incomplete canopy cover of cotton, Agricultural and Forest Meteorology. 46 (1989) 91–105. doi:10.1016/0168-1923(89)90114-7.

[32] G. Gosse, Profil de vent au-dessus d'un gazon en régime de neutralité thermique : détermination des coefficients d'échange, (1971). http://horizon.documentation.ird.fr/exl-doc/pleins_textes/divers11-05/06869.pdf.

[33] L.K. Balick, R.K. Scoggings, L.E. Link, Jr, Inclusion of a simple vegetation layer in terrain temperature

models for thermal infrared (IR) signature prediction, 1981. http://www.dtic.mil/dtic/tr/fulltext/u2/a104469.pdf.

[34] G.S. Campbell, J.M. Norman, An Introduction To Environmental Biophysics, Second Edition, Springer, 1998.

[35] J. Goudriann, Crop micrometeorology, 1977. http://edepot.wur.nl/166537.

[36] J.M. Norman, W.P. Kustas, K.S. Humes, Source approach for estimating soil and vegetation energy fluxes in observations of directional radiometric surface temperature, Agricultural and Forest Meteorology. 77 (1995) 263–293.